Influence of geometric and material nonlinearities on the behaviour and design of stainless steel frames

F. Walport[a], I. Arrayago[b], L. Gardner[a] and D.A. Nethercot[a]

[a]Department of Civil and Environmental Engineering, Imperial College London, London, UK

[b]Department of Civil and Environmental Engineering, Universitat Politècnica de Catalunya, Spain

E-mails: fiona.walport12@imperial.ac.uk, itsaso.arrayago@upc.edu, leroy.gardner@imperial.ac.uk, d.nethercot@imperial.ac.uk

Abstract: *Material nonlinearity affects the stiffness and consequently the distribution of internal forces and moments in indeterminate structures. This has a direct impact on their behaviour and design, particularly in the case of stainless steel, where material nonlinearity initiates at relatively low stress levels. A method for accounting for the influence of material nonlinearity in stainless steel frames, including making due allowance for the resulting amplified second order effects, is presented herein. Proposals have been developed for austenitic, duplex and ferritic stainless steels. The method was derived based on benchmark results calculated through second order inelastic analysis with strain limits, defined by the Continuous Strength Method, using beam finite element models. A comprehensive set of frames was modelled and the proposed assessment of second order effects in the plastic regime was also verified against the results of four full-scale stainless steel frame tests. The proposed method is due to be included in the upcoming revision to Eurocode 3 Part 1.4.*

Keywords: Continuous Strength Method; Frame stability; Global analysis; Inelastic analysis; Plastic design; Stainless steel; Strain limits.

1. INTRODUCTION

In the global analysis of structures, there are two key types of nonlinearity to consider: (1) geometric nonlinearity, also referred to as second order effects, and (2) material nonlinearity, also referred to as yielding or plasticity. The influence of both forms of nonlinearity have been extensively studied in isolation, but their interaction at system level has been less widely examined [1]; this is therefore the focus of the present paper, with an emphasis on stainless steel structures.

The influence of global second order effects is assessed in the Eurocode framework, based on the critical load factor of the system α_{cr}, which is the factor by which the applied loading would need to be increased to cause elastic instability of the frame in a global sway mode. Second order effects are deemed to be sufficiently small to be ignored when the amplification of the internal forces and moments due to sway second order effects is no more than 10% of the original internal forces determined according to first order theory – for elastic analysis, this corresponds to the requirement of $\alpha_{cr} > 10$ for second order effects to be neglected. Frames that experience plasticity suffer reduced stiffness and, therefore, have greater susceptibility to second order effects. This is accounted for in EN 1993-1-1 [2] by defining a stricter limit of $\alpha_{cr} > 15$ for second order effects to be ignored in plastically designed frames, but it was concluded in [3,4] that the use of a single limit is overly-simplistic and cannot reflect the behaviour of all structures, no matter the structural system or degree of plasticity. A new methodology to account for the degree of stiffness degradation in the assessment of second order effects was therefore proposed [3,4]. This initial research is further developed herein and extended to cover all three main families of stainless steel as well as a range of structural systems.

2. EUROCODE 3 DESIGN PROVISIONS

EN 1993-1-1 [2] allows for the use of elastic global analysis in all cases. It is deemed sufficient to carry out a first order analysis, ignoring the influence of second order effects, if the amplification of the internal forces and moments due to sway second order effects is no more than 10% of the original internal forces. This assessment of the stability of structural frames is made based on the critical load factor α_{cr}. For elastic analysis, this corresponds to a limit of $\alpha_{cr} \geq 10$, while for plastic analysis, a stricter limit of $\alpha_{cr} \geq 15$ is required allowing for the influence of plasticity and hence reduced stiffness on the development of second order effects. When α_{cr} is less than these limits, global second order effects must be considered. As a simplified approach, for elastic analysis, if $\alpha_{cr} > 3$ an amplified first order analysis using the amplification factor k_{amp}, given by Equation (1), may be carried out.

$$k_{\mathrm{amp}} = \frac{1}{1 - \frac{1}{\alpha_{\mathrm{cr}}}} \tag{1}$$

EN 1993-1-4 [5] provides supplementary rules for the design of stainless steel structures that extend and modify the design rules given for carbon steel in EN 1993-1-1 [2]. No further guidance is provided in EN 1993-1-4 for the global analysis of stainless steel structures, except to state that the use of plastic global analysis is not permitted. This restriction is due to be relaxed though for austenitic and duplex stainless steel in the upcoming revision to EN 1993-1-4, following the findings presented in [6,7].

A revised approach to the assessment of second order effects when a plastic analysis is performed is included in the upcoming version of prEN 1993-1-1 [8] based on research carried out by Wood [9]. In this approach, a reduced critical load factor to account for the increased susceptibility to second order effects due to plasticity is calculated by carrying out a linear buckling analysis of the elastic system, but with hinges at the locations of the plastic hinges.

The limit on α_{cr} of 10 from elastic analysis is retained for plastic analysis. The number and location of the hinges to be considered correspond either to (1) the plastic hinges formed just prior to reaching a collapse mechanism (i.e. when the penultimate plastic hinge forms), or, more accurately, to (2) the plastic hinges formed at the load level of interest [4].

The provisions of prEN 1993-1-1 [10] for assessing second order effects in the plastic regime only apply to plastic hinge analysis. However, idealised plastic hinges do not provide an accurate reflection of the development of plasticity in stainless steel structures owing to the rounded stress-strain response, which contrasts the sharply-defined yield point that is characteristic of hot-rolled carbon steel [1]. Consequently this method is not well suited to structural stainless steel design. Additionally, the approach can result in very conservative predictions since it assumes that the stiffness reduction due to the formation of plastic hinges begins from the onset of loading [4].

3. FINITE ELEMENT MODELLING

Finite element (FE) modelling is undertaken in order to investigate the influence of geometric and material nonlinearities on the behaviour and design of stainless steel frames. Figure 1 illustrates the comprehensive set of frames considered in this study, while Table 1 reports the boundary conditions, horizontal load cases, storey heights and bay widths considered for each of the frame cases analysed. In total, 279 frames were modelled (93 austenitic, 93 duplex and 93 ferritic stainless steel frames) to cover a full range of boundary conditions, load cases and frame geometries. Geometrically and materially nonlinear analysis with imperfections (GMNIA) allows for accurate predictions of the full global behaviour of a structure and is used herein to calculate the benchmark failure load for each frame α_u, as outlined in Section 3.3. Additionally, first (MNA) and second (GMNA) order plastic analyses (i.e. without member imperfections) are utilised to isolate the influence of the geometric and material nonlinearities, as outlined in Section 3.4.

All models were developed using the general-purpose FE software ABAQUS [11]. The assessed frames were formed from welded stainless steel I-sections with the cross-section geometry of a standard European HEB 340 cross-section. This cross-section is Class 1 for all stainless steel grades and loading conditions considered herein; it is therefore able to reach and maintain its full plastic moment capacity. All members in the frames were connected via fixed multi-point constraint ties to provide full continuity, and the systems were fully restrained out-of-plane such that only in-plane major axis bending/buckling was considered. 100 B31OS beam elements were used to model each of the members [3,12] and the modified Riks method [11] was used to trace the full load-deformation response of the frames. For each frame, the elastic critical load factor α_{cr} was determined by performing linear buckling analysis at the load level corresponding to failure of the system α_u, as calculated in Section 3.3.

3.1. Material modelling

Stainless steel alloys present a rounded stress–strain curve, which can be described by the two-stage Ramberg–Osgood material model [13–16]. This model is given by Equations (2) and (3), and is due to be included in prEN 1993-1-14 [17], where ε and σ are the strain and stress respectively, f_y is the yield (0.2% proof) stress, E is the Young's modulus, f_u is the ultimate stress, E_y is the tangent modulus at the yield (0.2% proof) stress, defined by Equation (4), $\varepsilon_{0.2}$ is the total strain at the 0.2% proof stress, equal to 0.002 + f_y/E, ε_u is the ultimate strain, and n and m are the strain hardening exponents.

$$\varepsilon = \frac{\sigma}{E} + 0.002\left(\frac{\sigma}{f_y}\right)^n \quad \text{for} \quad \sigma \le f_y \tag{2}$$

$$\varepsilon = \varepsilon_{0.2} + \frac{\sigma - f_{\mathrm{y}}}{E_{\mathrm{y}}} + \left(\varepsilon_{\mathrm{u}} - \varepsilon_{0.2} - \frac{f_{\mathrm{u}} - f_{\mathrm{y}}}{E_{\mathrm{y}}}\right)\left(\frac{\sigma - f_{\mathrm{y}}}{f_{\mathrm{u}} - f_{\mathrm{y}}}\right)^{m} \quad \text{for} \quad f_{\mathrm{y}} < \sigma \leq f_{\mathrm{u}} \tag{3}$$

$$E_{\mathrm{y}} = \frac{E}{1 + 0.002n\frac{E}{f_{\mathrm{y}}}} \tag{4}$$

The standardised material properties for numerical parametric studies defined by Afshan et al. [18] for the three main families of stainless steel used in construction – austenitic, duplex and ferritic – were employed in this study; the key material parameters adopted for each stainless steel family are summarised in Table 2.

3.2. Geometric imperfections and residual stresses

An initial member out-of-straightness in the form of a half-sine wave and with a magnitude of 1/1000 of the member length was modelled for all columns, while the initial frame out-of-plumbness was applied as an equivalent horizontal force equal to 1/200 times the vertical loading [2] at each storey load.

The residual stress distribution for welded stainless steel I-sections proposed by Yuan et al. [19] was incorporated into the benchmark FE models through the SIGINI user subroutine [11]. The flanges and web of the cross-section were each assigned 41 section points across their width to ensure that the residual stress distribution was accurately represented.

3.3. Benchmark failure loads α_{u}

In this study, benchmark failure loads were calculated through second order inelastic analysis (i.e. geometrically and materially nonlinear) with imperfections (GMNIA), performed using beam finite elements. Strain limits, determined from the Continuous Strength Method (CSM) [20–23], were applied to the outer-fibre compressive strains $\varepsilon_{\mathrm{Ed}}$ of each element in the frame, to simulate cross-section, and hence structural, failure [20]. The benchmark failure load α_{u}, was defined as the load level at which the CSM strain limit was reached or, in stability governed cases, as the peak load reached during the GMNIA analysis, whichever occurred first [3]. This method of design by second order inelastic analysis is due to be included in the upcoming prEN 1993-1-4 [10], prEN 1993-1-14 [17] and AISC 370 [24].

For the global analysis of stainless steel structures, utilising the Ramberg–Osgood material model, the CSM strain limits are calculated using Equations (5) and (6) for stocky and slender cross-sections, respectively:

$$\frac{\varepsilon_{\mathrm{csm}}}{\varepsilon_{\mathrm{y}}}=\frac{0.25}{\bar{\lambda}_{\mathrm{p}}^{3.6}}+\frac{0.002}{\varepsilon_{\mathrm{y}}} \quad \text{but} \;\leq \Omega \text{ for } \;\bar{\lambda}_{\mathrm{p}} \leq 0.68 \tag{5}$$

$$\frac{\varepsilon_{\mathrm{csm}}}{\varepsilon_{\mathrm{y}}}=\left(1-\frac{0.222}{\bar{\lambda}_{\mathrm{p}}^{1.05}}\right)\frac{1}{\bar{\lambda}_{\mathrm{p}}^{1.05}}+\frac{0.002\left(\sigma/f_{\mathrm{y}}\right)^{n}}{\varepsilon_{\mathrm{y}}} \quad \text{for } \;0.68<\;\bar{\lambda}_{\mathrm{p}} \leq 1.0 \tag{6}$$

where $\bar{\lambda}_{\mathrm{p}}$ is the local cross-sectional slenderness defined in Section 3.3.1, σ is the maximum compressive stress at the considered cross-section, n is the strain hardening exponent defined in Section 3.1, ε_{y} is the yield strain equal to the yield (0.2% proof) stress f_{y} divided by the Young's modulus E, and ε_{u} is the ultimate strain, estimated as $\varepsilon_{\mathrm{u}} = 1 - f_{\mathrm{y}}/f_{\mathrm{u}}$ for austenitic and duplex stainless steels and as $\varepsilon_{\mathrm{u}} = 0.6(1 - f_{\mathrm{y}}/f_{\mathrm{u}})$ for ferritic stainless steels, where f_{u} is the ultimate stress [25,26]. The limit of Ω defines an upper bound to the normalised CSM strain limit and was taken as equal to 15 in this study [21].

To account for the positive influence of local moment gradients, the CSM strain limit was applied to an average strain obtained over a characteristic length along the members. This characteristic length was taken equal to the elastic local buckling half-wavelength of the cross-section $L_{\mathrm{b,cs}}$, as discussed in Section 3.3.2. The instantaneous CSM strain limit $\varepsilon_{\mathrm{csm}}$, based on the instantaneous stress distribution within the section under consideration at each loading increment of the global structural analysis, was used as the limiting strain throughout this study. Note that since forces and moments within a system are redistributed during loading due to both member buckling and/or the spread of plasticity, the stress distribution across the cross-sections may change as the load level increases and hence, the location of the critical cross-section may also change throughout the loading history of the structure. It is therefore necessary to assess all cross-sections in the structure at each loading step.

3.3.1. Cross-section slenderness $\bar{\lambda}_{\mathrm{p}}$

The cross-section slenderness $\bar{\lambda}_{\mathrm{p}}$ is calculated using Equation (7) and quantifies the susceptibility of a cross-section to local buckling, where $\sigma_{cr,cs}$ is the local elastic critical buckling stress of the full cross-section.

$$\bar{\lambda}_{\mathrm{p}} = \sqrt{\frac{f_{\mathrm{y}}}{\sigma_{\mathrm{cr,cs}}}} \tag{7}$$

The elastic critical buckling stress $\sigma_{cr,cs}$ can be calculated using numerical methods, such as the finite strip method utilised in CUFSM [27], or alternatively approximate analytical expressions [28,29]; CUFSM was employed in the present paper.

3.3.2. Local buckling half-wavelength $L_{b,cs}$

The CSM strain limit is applied to an average strain obtained over the local buckling half-wavelength $L_{b,cs}$ [21] in order to take account of the beneficial effects of local moment gradients. As for the elastic critical buckling stress $\sigma_{cr,cs}$, the elastic local buckling half-wavelength $L_{b,cs}$ may be determined numerically or according to the expressions defined in [30]; in this study, CUFSM was used to estimate $L_{b,cs}$, with a value of $L_{b,cs}$ = 580 mm determined for the studied cross-section under pure bending.

3.4. First and second order plastic collapse load factors

The first order plastic collapse load factor α_{p1} is calculated through a first order plastic (or materially nonlinear) analysis (MNA), while the second order plastic collapse load factor α_{p2}

is calculated through a second order plastic (geometrically and materially nonlinear) analysis (GMNA). As for the benchmark ultimate loads in Section 3.3, the CSM strain limits were used to define cross-section failure. Note that for the first order analyses, since global instability effects are not captured, the strain limits govern failure of the frames in all cases.

4. INFLUENCE OF ROUNDED STRESS-STRAIN RESPONSE ON INTERNAL FORCES AND MOMENTS

As discussed in Section 2, the current frame stability design provisions for stainless steel follow those for carbon steel, with elastic global analysis allowed in all cases. While this is appropriate for carbon steel, which is accurately characterised by an elastic, perfectly plastic stress–strain response, it is less suitable for stainless steel, owing to the rounded nature of the stress–strain curve. The guidance on material nonlinearities in EN 1993-1-1 is based predominately on the occurrence of idealised plastic hinges. Again, while this is appropriate for carbon steel structures, in stainless steel structures, due to the rounded stress–strain response, idealised plastic hinges do not occur and instead, zones of plasticity with gradually reducing stiffness are displayed.

The degradation of stiffness due to material nonlinearity, which occurs at relatively low stress levels for stainless steel, can significantly affect the behaviour of a structural system and consequently, the distribution of internal forces and moments [4]. It is therefore important that an elastic global analysis is only permitted when all members contributing to the global stability of the structure remain predominately elastic under the design loading and when the loss of stiffness due to material nonlinearity has a negligible effect on the internal forces. In cases where the stiffness reduction due to the material nonlinearity of stainless steel increases the action effects significantly or modifies significantly the structural behaviour, it is necessary to perform a plastic zone analysis.

Figure 2 shows the ratio of bending moments obtained from first (M_{LA}) and second order (M_{MNA}) plastic zone analyses using the two-stage Ramberg–Osgood material model [13] of an example austenitic stainless steel single-bay single-storey portal frame with fixed-ended support conditions plotted against the ratio of the secant modulus E_s to elastic modulus E of the most heavily stressed point of the frame under increasing load levels. Depending on the location of the analysed cross-section within the frame and the design load level, ignoring material nonlinearity can results in both over-estimations ($M_{MNA}/M_{LA} < 1$) and under-estimations ($M_{MNA}/M_{LA} > 1$) of internal bending moments (and internal forces). When the ratio of E_s/E is less than 0.2, these differences approach 10%; the simplification of assuming that the behaviour of the structure remains elastic at all stress levels is not appropriate (taking 10% as the approximate acceptable error threshold, as for the case of second order effects) beyond this corresponding stress level. Although the percentage error will vary between frames and load combinations, as seen in Figure 3, which shows the maximum ratio of internal moments obtained from a first order plastic (MNA) and elastic (LA) analysis for 21 austenitic stainless steel portal frames (Frame case 1a), there is clear justification for the need to consider material nonlinearity in the global analysis of stainless steel frames to avoid unsafe predictions of internal forces and moments. It is recommended herein that if Equation (8) – also shown in Figures 2 and 3 – is satisfied, then an elastic analysis is acceptable; if Equation (8) is not satisfied, Equation (9) applies and the effects of material nonlinearity are significant enough to require a plastic zone analysis.

$$\text{If } \frac{E_s}{E} > 0.2\text{, elastic analysis is acceptable} \tag{8}$$

$$\text{If } \frac{E_s}{E} \leq 0.2\text{, plastic zone analysis is required} \tag{9}$$

In Equations (8) and (9), E_s is the secant modulus corresponding to the maximum stress σ_{Ed}, obtained from a first order elastic analysis in the cross-section of any member contributing to the global stability of the structure at the design load level, as calculated using Equation (10).

$$E_{\mathrm{s}} = \frac{E}{1 + 0.002\frac{E}{\sigma_{\mathrm{Ed}}}\left(\frac{\sigma_{\mathrm{Ed}}}{f_{\mathrm{y}}}\right)^{n}} \tag{10}$$

5. INFLUENCE OF PLASTICITY ON SECOND ORDER EFFECTS

In the elastic regime, second order effects may be approximately accounted for by either amplifying the internal moments or by reducing the ultimate load of a first order analysis. The amplification factor k_{amp}, as given by Equation (1), may be used to amplify horizontal loads to provide an estimate for the influence of second order effects, while the reduction factor (α_{e2}/α_{e1}), as defined by the Merchant–Rankine formula [31,32] given by Equation (11), may be used to reduce the failure load factor obtained from a first order elastic analysis and design checks α_{e1} to allow for second order effects to give α_{e2}.

$$\left(\frac{\alpha_{\mathrm{e2}}}{\alpha_{\mathrm{e1}}}\right) = \frac{\alpha_{\mathrm{cr}} - 1}{\alpha_{\mathrm{cr}}} \tag{11}$$

As concluded in [3,4], in the elastic regime, these expressions apply at all load levels and accurately relate the results of first and second order analyses. However, in the plastic regime these expressions are no longer sufficient and must instead be based on a reduced critical load factor. This is illustrated in Figures 4 and 5 for the 279 frames assessed herein. In Figure 4, the amplification factors k_{amp} for each frame are plotted against the elastic buckling load factors α_{cr}, as well as the expression for predicting the amplification of the horizontal loads given by Equation (1). Note that the amplification factors k_{amp} for the frames were calculated by determining the magnitude of the amplification of the horizontal loading in a first order plastic analysis (MNA) required to align the sway deflections to those in a second order plastic analysis (GMNA) at the benchmark ultimate load factor α_u, following the procedure detailed in [3]. The results in Figure 4 do not match well with the elastic amplification factor and lie on the unsafe side of the curve (by 15% on average and by up to almost 80% for particular cases). In all cases, at the limit of α_{cr} = 15, where second order effects are currently deemed in EN 1993-1-1 [2] (and by extension in EN 1993-1-4 [5]) to be sufficiently small to ignore, the amplification of the internal forces and moments due to sway second order effects is significantly more than 10% of the internal forces according to first order theory. Similar results can be seen in Figure 5, which shows the ratios of the second order plastic (GMNA) collapse load factor α_{p2} to the first order plastic (MNA) collapse load factor α_{p1}, alongside the Merchant–Rankine formula (Equation (11)), against the elastic critical load factors α_{cr}. The FE results do not match well with the reduction factor predicted by Equation (11) and the majority of the points lie on the unsafe side relative to the Merchant–Rankine formula, with an average value of $(\alpha_{p2}/\alpha_{p1})/((\alpha_{cr}-1)/\alpha_{cr})$ = 0.95 and a minimum value of 0.72. The results shown in these two figures clearly illustrate the need for the definition of a modified elastic buckling load factor $\alpha_{cr,mod}$ to account for the loss of stiffness due to material nonlinearities and second order effects.

The influence of material nonlinearity on the sway stiffness of frames may be considered through the modified elastic buckling load factor $\sigma_{cr,mod}$, as derived in [3,4], and given by Equation (12), where α_{cr} is the elastic buckling load factor, calculated through a linear buckling analysis at the applied load level and K_s/K is the ratio of the secant lateral stiffness K_s at the design value of the loading on the structure (as obtained from a first order plastic zone analysis) to the initial lateral stiffness K of the structure. As discussed in [3,4], it is not possible to predict from a first order analysis whether, at a given load level, additional plastification will occur due to second order effects. Therefore, as well as the secant stiffness reduction factor, an additional factor Y is needed to approximate the further loss of stiffness due to second order effects.

$$\alpha_{\mathrm{cr,mod}} = Y\frac{K_{\mathrm{s}}}{K}\alpha_{\mathrm{cr}} \tag{12}$$

Based on this modified load factor $\alpha_{\mathrm{cr,mod}}$, a modified amplification factor $k_{\mathrm{amp,mod}}$, as given by Equation (13), and a modified reduction factor $(\alpha_{\mathrm{p2}}/\alpha_{\mathrm{p1}})_{\mathrm{mod}}$, as given by Equation (14) may be defined for use in the plastic regime, where α_{p2} is the predicted second order plastic (GMNA) collapse load factor and α_{p1} is the first order plastic (MNA) collapse load factor.

$$k_{\mathrm{amp,mod}} = \frac{1}{1-\frac{1}{\alpha_{\mathrm{cr,mod}}}} \tag{13}$$

$$\left(\frac{\alpha_{\mathrm{p2}}}{\alpha_{\mathrm{p1}}}\right)_{\mathrm{mod}} = \frac{\alpha_{\mathrm{cr,mod}}-1}{\alpha_{\mathrm{cr,mod}}} \tag{14}$$

By accounting for the influence of plasticity on second order effects through the reduction of the critical load factor, as in prEN 1993-1-1 [8,9], the limit of 10 may be used for plastic analysis, as for elastic analysis. When $\alpha_{\mathrm{cr,mod}} \geq 10$, it may be assumed that second order effects are sufficiently small to be ignored and a first order analysis is adequate, while for $\alpha_{\mathrm{cr,mod}} < 10$, second order effects must be considered in the analysis, as they may be significant.

For multi-storey structures, the effects of material nonlinearity on the reduction in global sway stiffness should be assessed on a storey-by-storey basis, as illustrated in Figure 6. The storey that gives the greatest secant stiffness reduction (i.e. the lowest value of K_{s}/K) should be taken as the most critical storey and used to represent the overall frame; in Figure 6, this is the bottom storey. This prevents the deleterious influence of plasticity on frame stability from being 'averaged out' through the inclusion of the displacements of the storeys in which less plasticity occurs, thereby ensuring safe sided estimates of $\alpha_{\mathrm{cr,mod}}$.

Table 3 presents the Y factors derived in this study for the 279 austenitic, duplex and ferritic stainless steel frames assessed herein. The lower values of Y for austenitic stainless steel, increasing for duplex and ferritic stainless steels reflects the greater degree of roundedness of the stress-strain response and hence the earlier material softening and greater second order effects. The lower Y values for the more complex frames reflect the fact that with increased complexity the potential for more plasticity and redistribution, at a given load level, between a first order and second order analysis, is greater. The Y factors proposed for ferritic stainless steel alloys in Table 3 are equal to the factors derived in [3,4] for carbon steel frames; this reflects the fact that ferritic stainless steel has the least rounded stress-strain response among the considered stainless steel families and most closely matches the behaviour of carbon steel. It is also worth noting that the proposed Y factors for single storey frames for the different stainless steel families are similar to the ratio of the 0.05% proof stress $\sigma_{0.05}$ to the 0.2% proof (or yield) stress f_y, noting that the $\sigma_{0.05}/f_y$ ratio is linked to the degree of roundedness of the stress-strain curve, with lower $\sigma_{0.05}/f_y$ values signifying greater roundedness; the 0.05% proof stress corresponds to the stress at which a relatively small plastic strain of 0.05% is reached, so represents approximately the limit of proportionality in stainless steels [13]. The $\sigma_{0.05}/f_y$ ratios (based on the material properties selected herein, as reported in Table 2) are equal to 0.81 (= 250/310), 0.86 (= 456/530) and 0.92 (= 295/320) for the austenitic, duplex and ferritic grades, respectively.

Figures 7 and 8 show the amplification factors k_{amp} and ratios of the second order plastic (GMNA) collapse load factor α_{p2} to the first order plastic (MNA) collapse load factor α_{p1}, respectively, now plotted against the proposed modified elastic buckling load factor $\alpha_{cr,mod}$, calculated from Equation (12), with the Y factors reported in Table 3 for all frames considered in this study. Good agreement is seen between the results and the amplification factor and reduction factor, respectively. Note that the anomalous results in Figure 7 that lie substantially above the curve are due to the non-sway effects being significant; when non-sway effects are significant, amplifying the horizontal loads in a first order plastic analysis will not result in the same forces and moments in a corresponding second order plastic analysis [4,33].

The proposed modified critical load factor $\alpha_{cr,mod}$ for assessing the severity of second order effects on global stability provides accurate results and, through the secant stiffness reduction K_s/K, allows a rational assessment of the influence of material nonlinearity to be performed on a frame-by-frame basis depending on the level of plastic deformation under the applied load level. When $\alpha_{cr,mod} \geq 10$, the amplification of the internal forces and moments due to sway second order effects (with suitable allowance for plasticity) is no more than 10% of the original internal forces according to first order theory, and a first order plastic analysis may be carried out. When $\alpha_{cr,mod} < 10$, second order effects (with suitable allowance for plasticity) significantly modify the structural behaviour and a second order plastic analysis must be carried out.

6. EXPERIMENTAL VALIDATION OF PROPOSED ASSESSMENT METHOD

Validation of the proposed method for assessing the influence of second order effects in the plastic domain against four full-scale stainless steel frame tests [34,35] is presented in this section. The tests were performed on austenitic stainless steel single-bay portal frames with rectangular hollow section members. The four frames had the same overall geometry (spans equal to 4 m and column heights equal to 2 m) but comprised different cross-sections, ranging from Class 1 to Class 4, and had varying boundary conditions at the supports, to allow for the assessment of different levels of interaction between second order effects, material nonlinearity and local buckling effects.

The frames were subjected to varying ratios of static horizontal-to-vertical loading throughout the tests. The loading was introduced in a two-step process: first the vertical loading was applied, then, while the vertical loading remained constant, the horizontal loading was increased. Consequently, the susceptibility of the frames to second order effects also varied as the horizontal loading was introduced. The effect of this variation in the loading ratio on the behaviour of the structure was investigated in [34,35] by considering two different ratios of loading in the calculation of the critical load factor: (1) the vertical load plus half of the maximum recorded horizontal load ($F_{v,max}+0.5F_{h,max}$), and (2) the vertical load plus the maximum recorded horizontal load ($F_{v,max}+1.0F_{h,max}$). The results in [34,35] showed that varying the horizontal-to-vertical load ratio had little effect on the calculated critical load factors. Therefore, only the results corresponding to the maximum horizontal loading scenario ($F_{v,max}+1.0F_{h,max}$) have been considered in the present paper.

To assess the accuracy of using the elastic critical load factor α_{cr} (as currently employed in EN 1993-1-1 [2] and EN 1993-1-4 [5]) to predict the amplification of internal moments (through the k_{amp} factor given by Equation (1)) and the reduction in ultimate load from a first order plastic analysis (through the α_{p2}/α_{p1} factor given by Equation (11)) due to second order effects, the experimental results, based on the maximum applied loads reported in [34,35], have been plotted in Figures 4 and 5. Note that, since some of the frames were made up of members with slender cross-sections, and consequently failure was dominated by local buckling effects, the first order plastic collapse loads were calculated using a shell FE second order analysis but with a horizontal force applied in the counter direction to remove the influence of global second order effects. In general, it can be seen that the experimental results show a similar trend to the FE data and both the k_{amp} and α_{p2}/α_{p1} predictions generally lie on the unsafe side. However, when $\alpha_{cr,mod}$ is used in place of α_{cr}, as shown in Figures 7 and 8, considerably better agreement between the experimental results and the predictive expressions – Equation (13) for $k_{amp,mod}$ and Equation (14) for $(\alpha_{p2}/\alpha_{p1})_{mod}$ – is achieved, as found for the numerical results. Thus, it can be concluded that use of the proposed modified critical load factor $\alpha_{cr,mod}$ enables the accurate assessment of the interaction of geometric and material nonlinearities (i.e. second order effects and plasticity) in stainless steel frames.

7. CONCLUSIONS

Degradation of stiffness due to material nonlinearity, which occurs at relatively low stress levels for stainless steel, can significantly affect the distribution of internal forces and moments in a structural system. It is therefore important that an elastic global analysis is only permitted when all members contributing to the global stability remain predominantly elastic under the design loading and when the loss of stiffness due to material nonlinearity has a negligible effect on the distribution of internal forces. A limit is proposed herein, expressed through the secant-to-Young's modulus ratio (E_s/E), to determine whether an elastic analysis is acceptable or the effects of material nonlinearity are significant enough to require a plastic zone analysis.

A second consequence of the degradation of stiffness due to material nonlinearity is enhanced second order effects. The influence of global second order effects is assessed in the Eurocode framework on the basis of the critical load factor of the system α_{cr}. A modified critical load factor $\alpha_{cr,mod}$ is proposed herein to assess the severity of second order effects on the global stability of stainless steel frames in the plastic regime. Through a secant stiffness reduction factor, the proposal allows a rational assessment of second order effects to be performed on a frame-by-frame basis depending on the level of plasticity experienced at the design load level. An additional factor Y accounts for the varying influence of material nonlinearity depending on the frame type and stainless steel family, with lower values (i.e. greater reductions in stiffness) employed for more complex frames and more rounded stress-strain curves. Second order effects are deemed to be sufficiently small to be ignored for cases in which the modified critical load factor $\alpha_{cr,mod} > 10$ i.e. the same limit as used for elastic analysis is retained. The applicability and accuracy of the proposed method is demonstrated through comparisons with numerical results on a comprehensive series of stainless steel frames, as well as test results from [34,35]. The findings and resulting proposals are consistent with those made in [4] for carbon steel frames and the proposed design method is due to be included in the upcoming version of prEN 1993-1-4 [10].

ACKNOWLEDGEMENTS

Funding for this investigation was received from the Imperial College PhD Scholarship scheme and the Engineering and Physical Sciences Research Council (EPSRC). The financial support provided by the Spanish Ministerio de Educación, Cultura y Deporte through the José Castillejo-2018 scholarship is also acknowledged.

REFERENCES

[1] Gardner, L. 2019. Stability and design of stainless steel structures – Review and outlook. *Thin-Walled Structures*, 141: 208–16.

[2] EN 1993-1-1. 2005. Eurocode 3: Design of steel structures - Part 1-1: General rules and rules for buildings. Brussels: CEN; 2005.

[3] Walport, F., Gardner, L., Real, E., Arrayago, I., & Nethercot, D.A. 2019. Effects of material nonlinearity on the global analysis and stability of stainless steel frames. *Journal of Constructional Steel Research*, 152: 173–82.

[4] Walport, F., Gardner, L., & Nethercot, D.A. 2019. A method for the treatment of second order effects in plastically-designed steel frames. *Engineering Structures*, 200: 109516.

[5] EN 1993-1-4:2006 + A1: 2015. Eurocode 3 - Design of steel structures - Part 1-4: General rules - Supplementary rules for stainless steels. Brussels: CEN; 2015.

[6] Theofanous, M., Saliba, N., Zhao, O., & Gardner, L. 2014. Thin-Walled Structures Ultimate response of stainless steel continuous beams. *Thin Walled Structures*, 83: 115–27.

[7] Arrayago, I., Real, E., & Mirambell, E. 2017. Design of stainless steel continuous beams

with tubular cross-sections. *Engineering Structures*, 151: 422–31.

[8] prEN 1993-1-1. 2020. Eurocode 3 – Design of steel structures – Part 1-1: General rules and rules for buildings. *CEN*,: Final Draft.

[9] Wood, R.H. 1958. The stability of tall buildings. *Proceedings of the Institution of Civil Engineers,*: 69–102.

[10] prEN 1993-1-4. 2020. Eurocode 3 - Design of steel structures - Part 1-4: General rules - Supplementary rules for stainless steels. *CEN*, Draft 2.

[11] ABAQUS. 2014. Abaqus CAE User's Manual, Version 6.14. Pawtucket, USA: Hibbitt, Karlsson & Sorensen, Inc.; 2014.

[12] Kucukler, M., Gardner, L., & Macorini, L. 2016. Development and assessment of a practical stiffness reduction method for the in-plane design of steel frames. *Journal of Constructional Steel Research*, 126: 187–200.

[13] Arrayago, I., Real, E., & Gardner, L. 2015. Description of stress-strain curves for stainless steel alloys. *Materials and Design*, 87: 540–52.

[14] Mirambell, E., & Real, E. 2000. On the calculation of deflections in structural stainless steel beams: an experimental and numerical investigation. *Journal of Constructional Steel Research*, 54: 109–33.

[15] Rasmussen, K.J.R. 2003. Full-range stress–strain curves for stainless steel alloys. *Journal of Constructional Steel Research*, 59: 47–61.

[16] Ramberg, W., & Osgood, W. 1943. Description of stress-strain curves by three parameters. *Technical Note No 902, National Advisory Committee For Aeronautics*,.

[17] prEN 1993-1-14. 2019. Eurocode 3 – Design of steel structures – Part 1-14: Design by FE analysis. *CEN*, Draft 1.

[18] Afshan, S., Zhao, O., & Gardner, L. 2019. Standardised material properties for numerical parametric studies of stainless steel structures and buckling curves for tubular columns. *Journal of Constructional Steel Research*, 152: 2–11.

[19] Yuan, H.X., Wang, Y.Q., Shi, Y.J., & Gardner, L. 2014. Residual stress distributions in welded stainless steel sections. *Thin-Walled Structures*, 79: 38–51.

[20] Walport, F., Gardner, L., & Nethercot, D.A. 2021. Design of structural stainless steel members by second order inelastic analysis with CSM strain limits. *Thin-Walled Structures*, 159: 107267.

[21] Fieber, A., Gardner, L., & Macorini, L. 2019. Design of structural steel members by advanced inelastic analysis with strain limits. *Engineering Structures*, 199: 109624.

[22] Fieber, A., Gardner, L., & Macorini, L. 2020. Structural steel design using second-order inelastic analysis with strain limits. *Journal of Constructional Steel Research*, 168: 105980.

[23] Quan, C., Kucukler, M., & Gardner, L. 2020. Design of web-tapered steel I-section members by second-order inelastic analysis with strain limits. *Engineering Structures*, 224: 111242.

[24] AISC. 2021. AISC 370. Specification for Structural Stainless Steel Buildings. Draft for public review. AISC; 2021.

[25] Afshan, S., & Gardner, L. 2013. The continuous strength method for structural stainless steel design. *Thin-Walled Structures*, 68: 42–9.

[26] Bock, M., Gardner, L., & Real, E. 2015. Material and local buckling response of ferritic stainless steel sections. *Thin-Walled Structures*, 89: 131–41.

[27] Li, Z., & Schafer, B.W. 2010. Buckling analysis of cold-formed steel members with

general boundary conditions using CUFSM: Conventional and constrained finite strip methods. *Proceedings Twentieth International Specialty Conference on Cold-Formed Steel Structures,*: 17–31.

[28] Gardner, L., Fieber, A., & Macorini, L. 2019. Formulae for calculating elastic local buckling stresses of full structural cross-sections. *Structures*, 17: 2–20.

[29] Quan, C., Fieber, A., & Gardner, L. 2021. Elastic local buckling of three-flanged cross-sections. *Thin-Walled Structures*, 160: 107251.

[30] Fieber, A., Gardner, L., & Macorini, L. 2019. Formulae for determining elastic local buckling half-wavelengths of structural steel cross-sections. *Journal of Constructional Steel Research*, 159: 493–506.

[31] Merchant, W. 1954. The Failure Load of Rigid Jointed Frameworks as Influenced by Stability. *The Structural Engineer*, 32: 185–90.

[32] Maquoi, R., & Jaspart, J.P. 2002. Merchant-Rankine Approach for the Design of Steel and Composite Sway Building Frames: 241–63.

[33] Demonceau, J.F., Ly, L., Comeliau, L., & Jaspart, J.P. 2010. New simplified analytical method for the prediction of global stability of steel and composite sway frames. *Structural Stability Research Council - Annual Stability Conference, SSRC 2010 - Proceedings,*: 1–20.

[34] Arrayago, I., González-de-León, I., Real, E., & Mirambell, E. 2020. Tests on stainless steel frames. Part I: Preliminary tests and experimental set-up. *Thin-Walled Structures*, 157: 107005.

[35] Arrayago, I., González-de-León, I., Real, E., & Mirambell, E. 2020. Tests on stainless steel frames. Part II: Results and analysis. *Thin-Walled Structures*, 157: 107006.

Table 1: Frame cases considered for each stainless steel family

Frame case No.	No. of frames	Boundary conditions	Horizontal loading H	Storey height(s) h [m]	Bay width(s) L [m]
1	21	Fixed	0.05V, 0.2V, 0.5V	5, 6, 7, 8, 9, 10, 15	10
2	7	Pinned	0.2V	5, 6, 7, 8, 9, 10, 15	10
3	6	Fixed	0.05V, 0.2V, 0.5V	5, 10	10
4	12	Fixed	0.05V, 0.2V, 0.5V	5, 8, 10, 15	10
5	3	Fixed	0.05V, 0.2V, 0.5V	5	10
6	3	Fixed	0.05V, 0.1V, 0.2V	5	10
7	6	Fixed	0.05V, 0.2V, 0.5V	5, 10	10
8	7	Fixed	0.2V	5, 6, 7, 8, 9, 10, 15	10
9	3	Fixed	0.1V, 0.2V, 0.41V	10	10
10	1	Fixed	0.2V	5	10
11	6	Fixed	0.05V, 0.2V, 0.5V	5, 10	10 - 5
12	6	Fixed	0.05V, 0.2V, 0.5V	5, 10	5 - 10
13	1	Fixed	0.13V	10	10
14	1	Pinned	0.13V	10	10
15	6	Fixed	0.13V, 0.2V	5, 8, 10	10
16	2	Fixed	0.13V, 0.27V	5	10
17	2	Fixed	0.2V, 0.5V	5	10

Table 2: Definition of material properties for parametric studies

Stainless steel family	E [N/mm^2]	f_y [N/mm^2]	f_u [N/mm^2]	ε_u [mm/mm]	n	m
Austenitic	200000	310	670	0.54	6.3	2.6
Duplex	200000	530	770	0.30	9.3	3.6
Ferritic	200000	320	480	0.16	17.2	2.8

Table 3: Proposed Y factors to account for the additional loss in stiffness

Stainless steel family	For single storey portal frames	For all other frames
Austenitic	0.80	0.55
Duplex	0.85	0.60
Ferritic	0.90	0.65

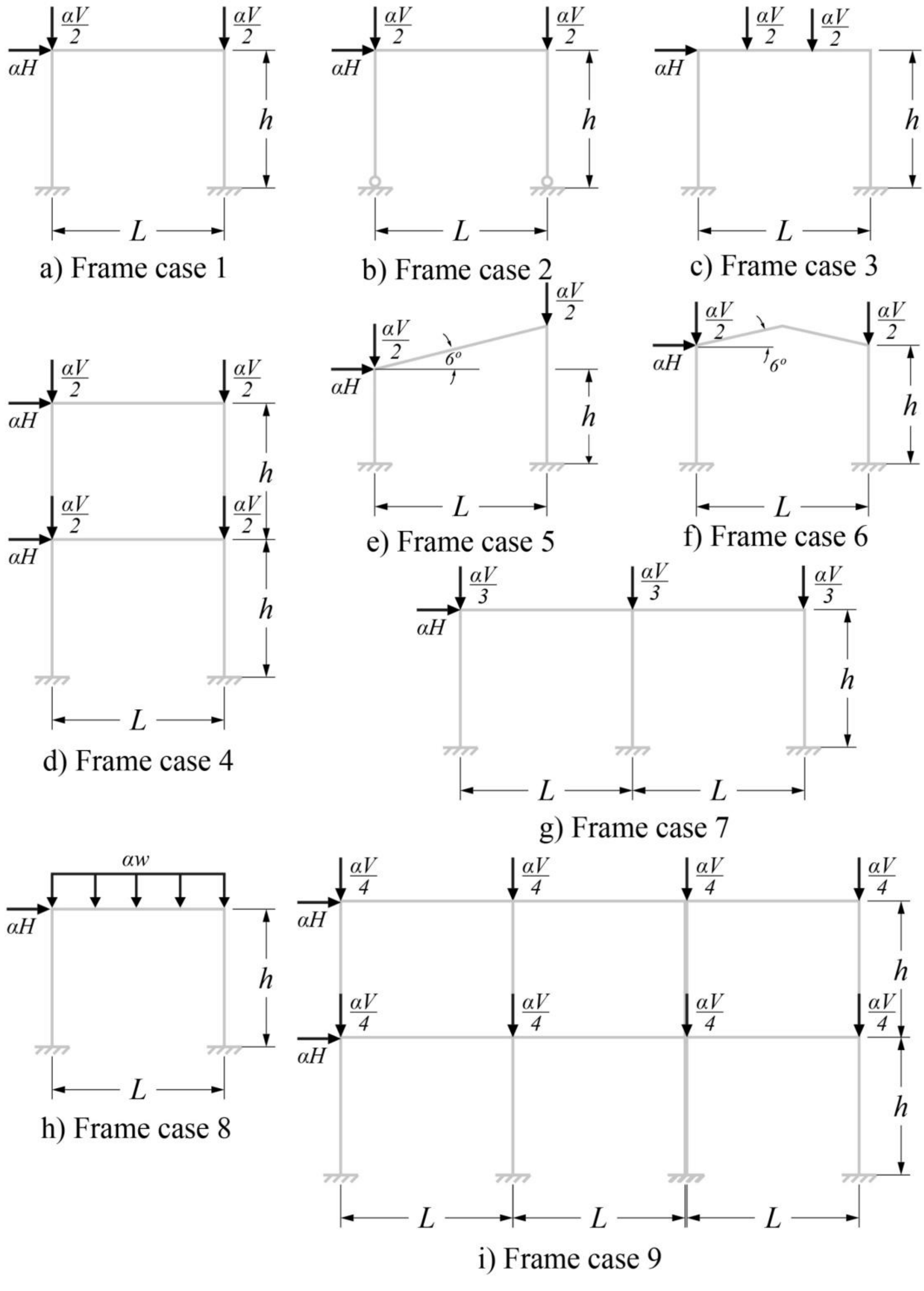

Figure 1: Details of modelled frames, where α is the load factor.

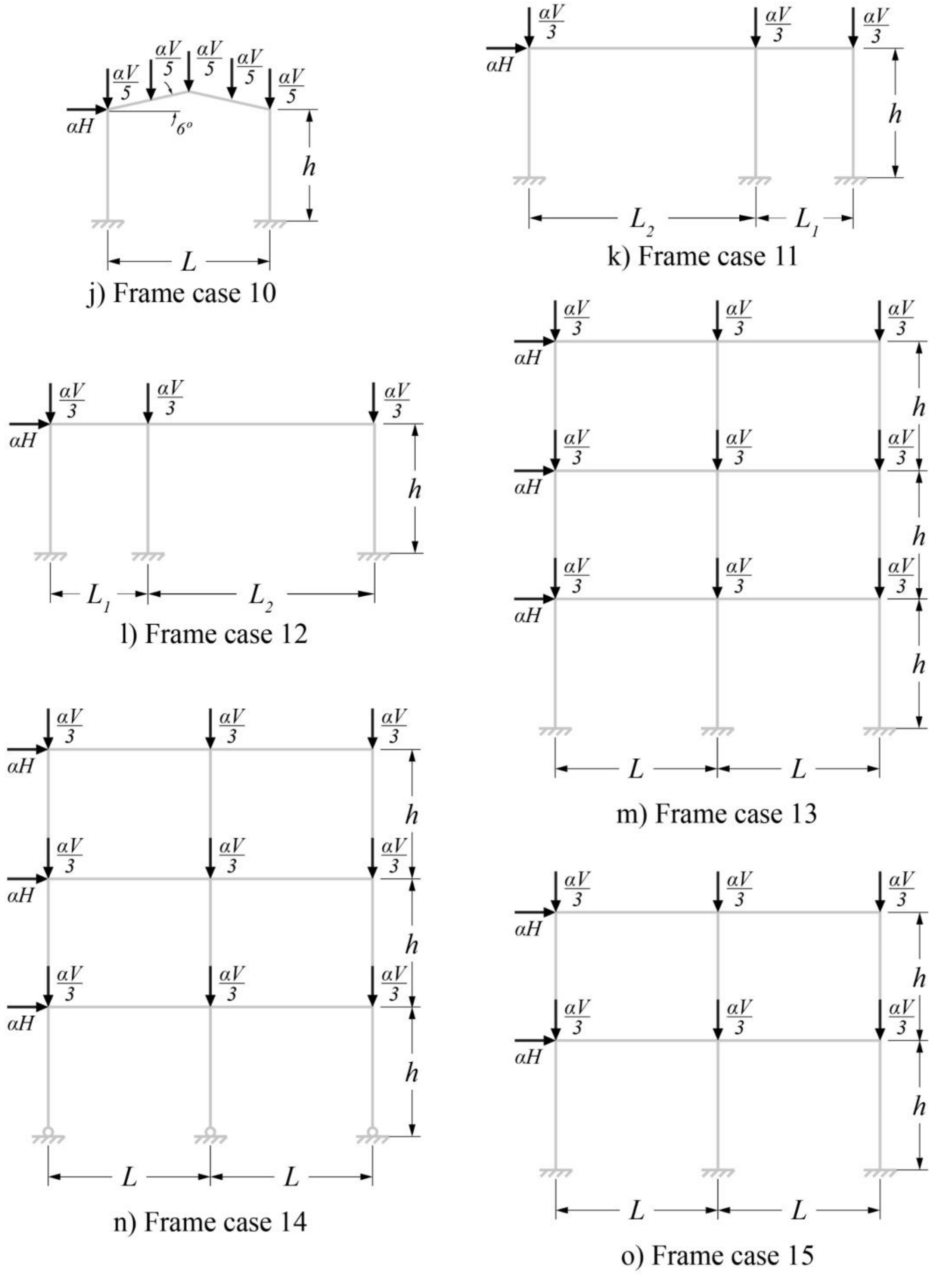

Figure 1 (cont.): Details of modelled frames, where α is the load factor.

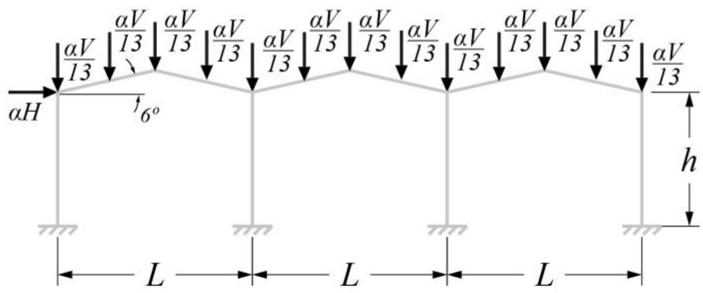

p) Frame case 16

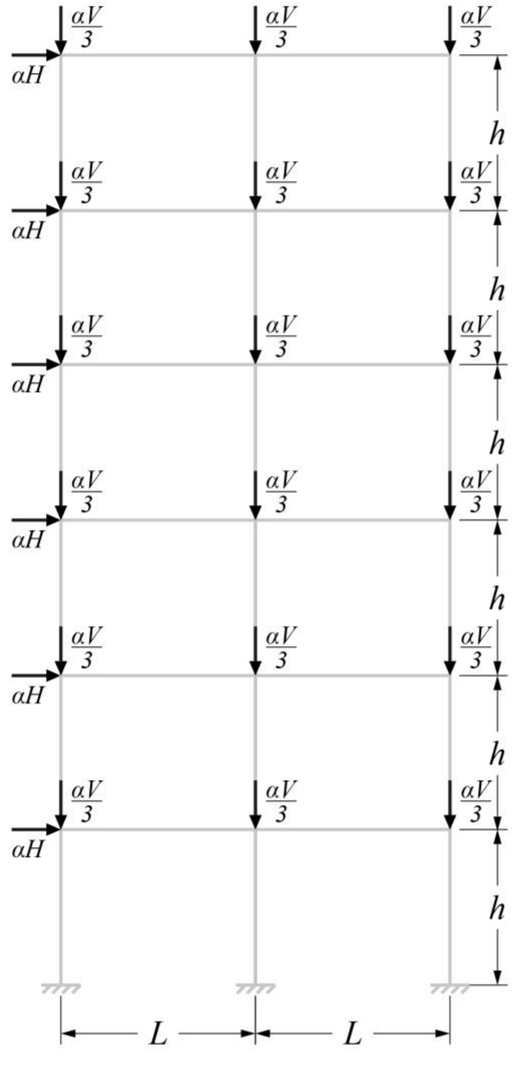

q) Frame case 17

Figure 1 (cont.): Details of modelled frames, where α is the load factor.

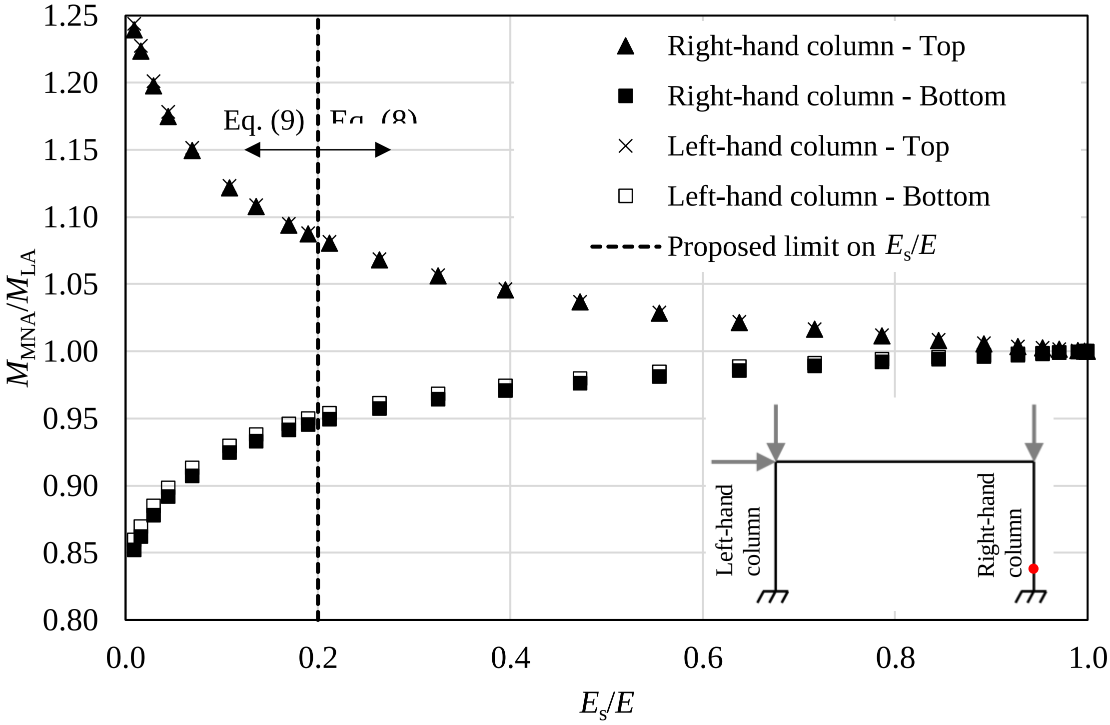

Figure 2: Ratio of internal moments obtained from a first order plastic (M_{MNA}) and elastic (M_{LA}) analysis at different locations in an example 5×10 m austenitic stainless steel portal frame plotted against the ratio of the secant modulus E_s to the elastic modulus E at the most heavily stressed point in the frame (as indicated by the red circle).

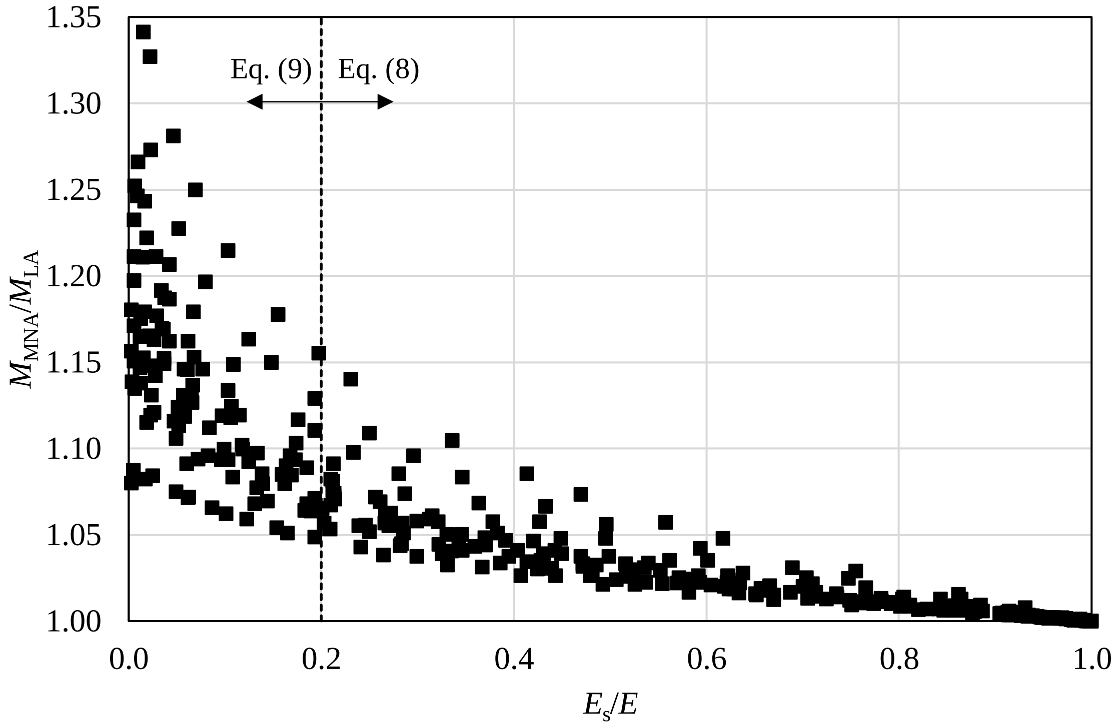

Figure 3: Maximum ratio of internal moments obtained from a first order plastic (M_{MNA}) and elastic (M_{LA}) analysis for 21 austenitic stainless steel portal frames (Frame case 1a) plotted against the ratio of the secant modulus E_s to the elastic modulus E at the most heavily stressed point in the frame.

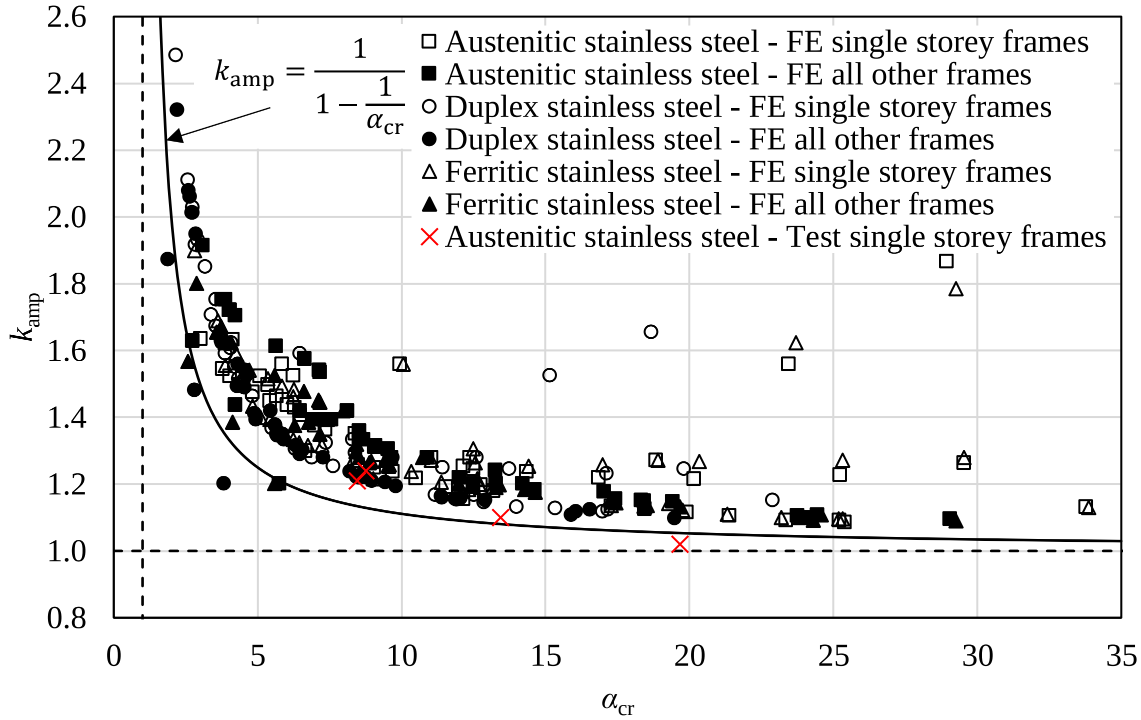

Figure 4: Amplification factor k_{amp} on the applied horizontal loading to obtain the same sway deflections from first (MNA) to second order plastic (GMNA) analyses at α_u versus α_{cr}. The predictive k_{amp} expression is based on α_{cr} and hence makes no allowance for material nonlinearity; as a consequence, the vast majority of results are on the unsafe side.

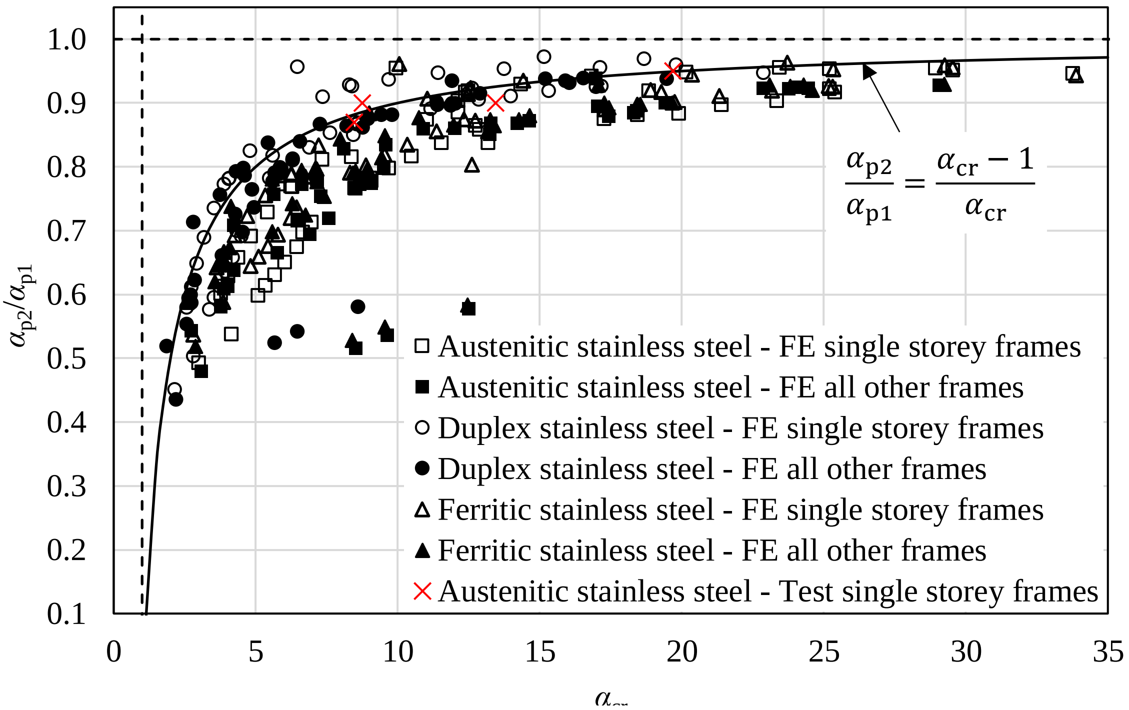

Figure 5: Ratio of second order plastic (GMNA) collapse load factor α_{p2} to first order plastic (MNA) collapse load factor α_{p1} versus α_{cr}. No allowance is made for material nonlinearity and the vast majority of results are on the unsafe side.

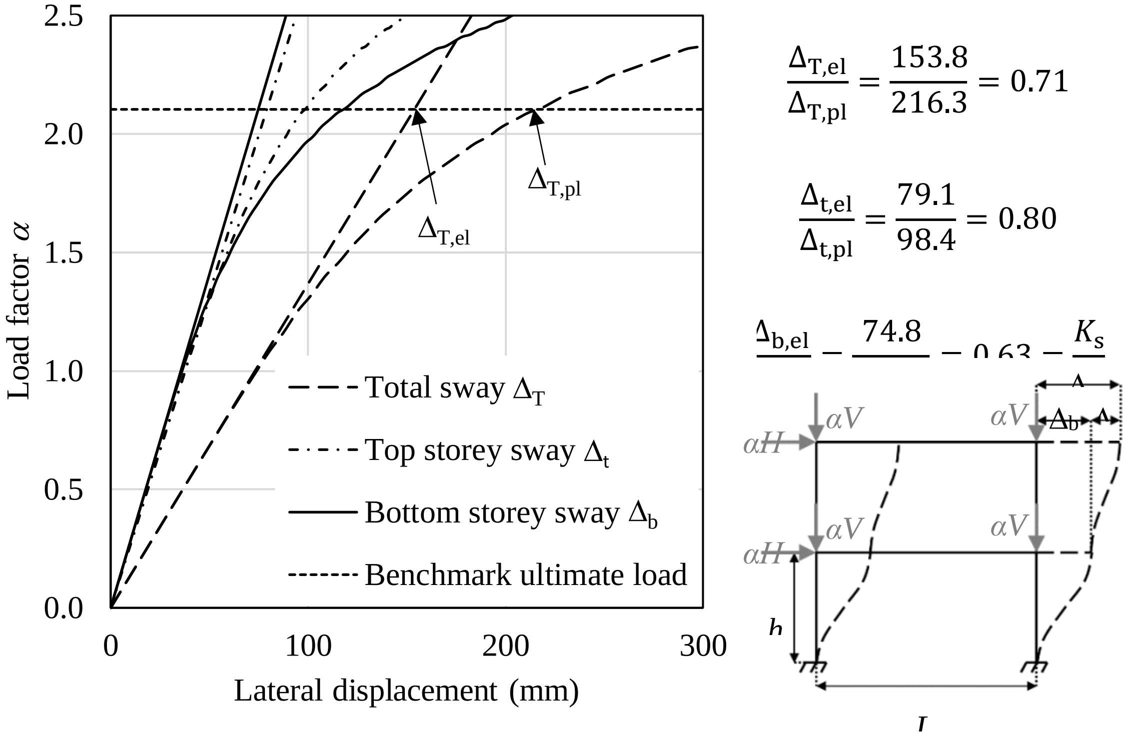

Figure 6: Example austenitic stainless steel two-storey frame where L=10 m and h = 5 m and H = 0.2V.

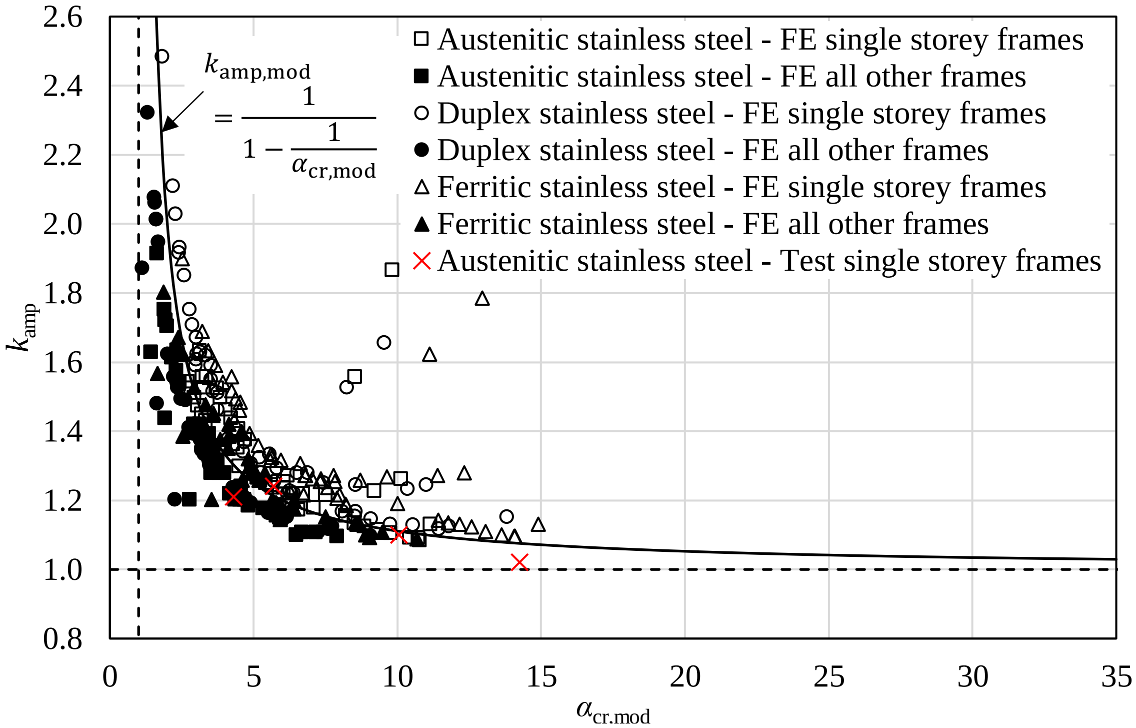

Figure 7: Amplification factor k_{amp} on the applied horizontal loading to obtain the same sway deflections from first (MNA) to second order plastic (GMNA) analyses at α_u versus $\alpha_{cr,mod}$; $\alpha_{cr,mod}$ is used to allow for the influence of material nonlinearity on frame stability.

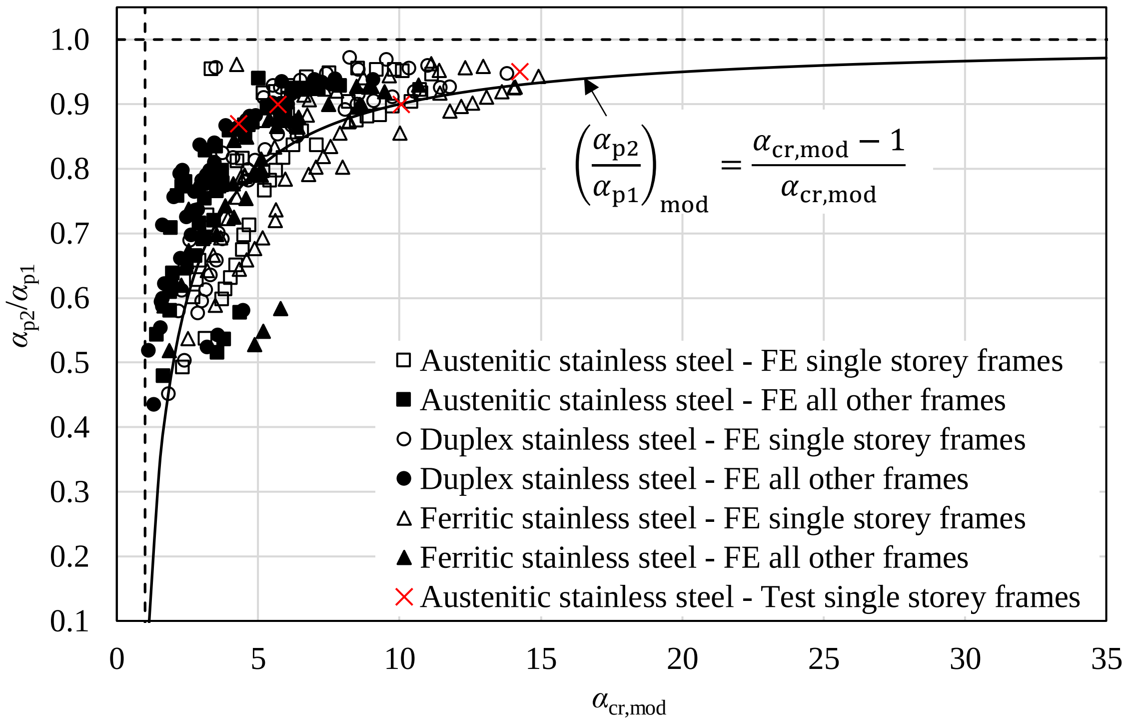

Figure 8: Ratio of second order plastic (GMNA) collapse load factor α_{p2} to first order plastic (MNA) collapse load factor α_{p1} versus $\alpha_{cr,mod}$; $\alpha_{cr,mod}$ is used to allow for the influence of material nonlinearity on frame stability.